

1 **Evaluating risk detection methods to uncover ontogenic-** 2 **mediated adverse drug effect mechanisms in children**

3 Authors:

4 Nicholas P. Giangreco^{1,2} and Nicholas P. Tatonetti^{1,*}

5 ¹Departments of Systems Biology and Biomedical Informatics, Columbia University, 622 W.
6 168th Street, New York, NY, 10032

7 ²npg2108@cumc.columbia.edu, ORCID: 0000-0001-8138-4947

8 *Correspondence: npt2105@cumc.columbia.edu, ORCID: 0000-0002-2700-2597

9 **Abstract**

10 **Background:** Identifying adverse drugs effects (ADEs) in children is essential for preventing
11 disability and death from marketed drugs. At the same time, however, detection is challenging
12 due to dynamic biological processes during growth and maturation, called ontogeny, that alter
13 pharmacokinetics and pharmacodynamics. As a result, current data mining methodologies have
14 been limited to event surveillance and have not focused on investigating adverse event
15 mechanisms. There is an opportunity to design data mining methodologies to identify and
16 evaluate drug event patterns within observational databases for ontogenic-mediated adverse
17 event mechanisms. The first step of which is to establish statistical models that can identify
18 temporal trends of adverse effects across childhood. **Results:** Using simulation, we evaluated a
19 population stratification method (the proportional reporting ratio or PRR) and a population
20 modeling method (the generalized additive model or GAM) to identify and quantify ADE risk at
21 varying reporting rates and dynamics. We found that GAMs showed improved performance over
22 the PRR in detecting dynamic drug event reporting across child developmental stages. Moreover,
23 GAMs exhibited normally distributed and robust ADE risk estimation at all development stages
24 by sharing information across child development stages. **Conclusions:** Our study underscores the
25 opportunity for using population modeling techniques, which leverages drug event reporting
26 across development stages, to identify adverse drug effect risk resulting from ontogenic
27 mechanisms.

28 **Keywords**

29 [Pharmacovigilance](#), [Pediatrics](#), [Child Development](#), [Modeling](#), [Dynamics](#)

30 **Background**

31 Adverse drug events (ADEs) in children are common and can result in injury and death^{1,2}.
32 Clinical trials rarely include children³ and pediatric-specific trials are limited in identifying
33 possible ADEs in the population⁴. Pediatric drug safety studies can evaluate large numbers of
34 ADEs from the population⁵ but current methodologies are limited in their ability to identify the
35 mechanisms that drive pediatric ADEs⁶. Children undergo evolutionarily conserved and
36 physiologically dynamic biological processes, collectively called ontogeny, as they grow and
37 develop from birth through adolescence^{7,8}. The mechanisms may include varying protein
38 activity^{9,10} as well as include functional and structural changes that occur during maturation^{11,12}.
39 These ontogenic changes can alter pharmacodynamics and pharmacokinetics resulting in adverse
40 effects, as is the case for doxorubicin-induced cardiotoxicity¹³ and valproate-induced
41 hepatotoxicity¹⁴. With a few notable exceptions, however, many pediatric adverse events are
42 idiopathic with no known, clear connection to developmental biology^{15,16}. Additionally, adverse
43 event mechanisms established in adults may not translate to the pediatric population¹⁷. There is
44 an opportunity to combine known ontogenic biology with real-world pediatric drug effect data to
45 identify ontogenic-mediated adverse events.

46 To date, elucidation of ontogenic mechanisms has relied on hypothesis-driven approaches. For
47 example, juvenile mouse models have been used to identify genetic vulnerabilities of
48 hematopoiesis¹⁸ and investigate effects by a glutamatergic agonist on the neural developmental
49 sequence¹⁹ during early life. More recently, pharmacometric tools have been used to extrapolate
50 drug effects from adults to children, such as projecting acetaminophen exposure across pediatric
51 age groups²⁰, and investigate drug action in children, such as predicting clearance of zidovudine

52 during infancy²¹. However, juvenile animal studies are low-throughput and require complex
53 study designs²², and there is limited experimental data to parameterize manually designed
54 pharmacometric models^{23,24}. While lacking specificity, top-down studies are complementary in
55 that they evaluate thousands of hypotheses simultaneously and can identify idiosyncratic effects
56 that would otherwise go unnoticed^{25,26}. Moreover, analyses of large population datasets start
57 from clinically significant events which can take decades to identify^{27,28}. Top-down studies can
58 close the pediatric evidence gap²³ by sifting through large databases to identify clinically
59 significant although perhaps less studied and rare adverse drug events during the period of child
60 growth and development.

61 While pediatric pharmacovigilance has been able to identify adverse drug events, it is limited in
62 identifying growth and development processes that underlie those observations^{10,29}. A common
63 approach when identifying ADEs is to stratify the pediatric population into age groups which
64 directly reduces the amount of data available to identify ADEs during childhood. The
65 Proportional Reporting Ratio, which was designed to be sensitive even when data is scarce³⁰, is
66 an established detection method and has been shown to unmask ADE signal within child
67 development stages compared to detection within the larger pediatric population³¹. However,
68 reduced data within these strata was shown to significantly affect PRR detection performance
69 across pediatric age groups³¹. To investigate pediatric ADEs, the continuous, time-dependent
70 biological processes during growth and development suggest using all information across child
71 development stages.

72 Generalized additive models (GAMs) are supervised machine learning approaches that can
73 quantify non-linear effects reflective of natural phenomena³². GAMs may be able to quantify
74 signal reflecting dynamic, continuous processes such as ontogeny. These models are extensively

75 used for spatial and temporal analysis in ecological studies³³, such as explaining cardiovascular
76 mortality risk from heat waves over time³⁴ and rat infestation from environmental factors within
77 geographic areas³⁵. Similar to evaluating ecological responses using shared information across
78 time or space, we can evaluate adverse events from temporally-connected ontogenic processes
79 using shared information across child development stages.

80 We performed the first study to directly evaluate dynamic drug event reporting during childhood.
81 We performed a data simulation and augmentation study that 1) simulated drug event reporting
82 temporal trends of different effect sizes and shapes, 2) augmented existing pediatric drug event
83 data by inserting the simulated reporting rates within observational data, and 3) evaluated
84 population stratification (PRR) and modeling (GAM) methods to detect these injected ADE
85 reporting dynamics. We found the detection scores generated by the GAM showed improved risk
86 estimates and increased detection of drug event reporting among the various simulated dynamics
87 compared to the PRR. Detection methods that capture temporal adverse drug event dynamics
88 within observational databases can improve our understanding of the interactions between child
89 developmental biology and adverse drug effects.

90 **Results**

91 *Pediatric FAERS*

92 There were 339,741 pediatric drug event reports in FAERS, which contained 519,555 unique
93 drug-event pairs. We randomly sampled 500 drug-event pairs to be augmented with simulated
94 drug event reporting dynamics, representing our positive control set. We then randomly sampled
95 another 10,000 complementary drug-event pairs where the underlying data was untouched,

96 representing our negative control set. We showed there was no significant difference in the
97 amount of drug-event reporting between FAERS and the negative control (2-sample Student t-
98 test p-value=0.92) or positive control (p-value=0.87) drug-event pairs (Figure 1).

99 *Data simulation and augmentation*

100 We augmented the 500 drug-event pairs in the positive control set with simulated drug event
101 reporting across child development stages (see Methods). Augmenting the positive control data
102 with drug event reporting dynamics did not have a systematic effect on the amount of drug event
103 reporting compared to the untouched negative control set (Figure S1). However, applying the
104 PRR and GAM detection methods onto the positive control data showed the ADE risk scores
105 reflected the simulated dynamics classes (Figure 2).

106
107 The GAM generated ADE risk that resembled normally distributed scores (Shapiro-Wilk test
108 average p-value and 95% confidence interval: 0.45 [0.059, 0.88], 90mse: 0.20 [4.67E-04, 0.92])
109 in comparison to the PRR (score: 0.11 [1.80E-09, 0.56], 90mse: 0.077 [2.48E-09, 0.93]) at child
110 development stages (Figure 3A). Moreover, 47% of PRR scores were zero and 18% were unable
111 to be computed, on average for drug-event pairs (Figure 3B).

112 *ADE dynamics detection performance*

113 We compared the performance of the GAM and PRR for detecting drug event reporting
114 dynamics (see Methods). Additionally, we further investigated the performance contribution by
115 each child development stage within the dynamics class. We found that the GAM had improved
116 detection of drug event reporting dynamics compared to the PRR both overall (Figure 4A) and
117 within each child development stage (Figure 4B). Moreover, the GAM had similar overall

118 performance (Figure 5) as well as sensitivity (Figure S3) at low drug event reporting compared
119 to the sensitive-by-design PRR.

120 *ADE dynamics sensitivity analysis*

121 We investigated the detection of drug event reporting dynamics with increasingly rare adverse
122 events within child development stages (Figure S4 and see Methods). The ADE risk scores
123 generated by the GAM showed dependent, flexible risk estimates across child development
124 stages unlike the PRR (Figure S5). We found that the GAM had significantly higher performance
125 (Figure 6) and sensitivity (Figure S5) to detect the various drug event reporting dynamics as
126 adverse events became rare at child development stages.

127 *Real-world validation*

128 We compared the performance of the GAM and PRR for detecting drug-event pairs in a real-
129 world pediatric reference set of 26 drug-event pairs (see Methods and Figure S6). We found that
130 the GAM had slightly improved overall performance and sensitivity compared to the PRR for
131 detecting pediatric adverse drug events (Table 1 and Figure S7). Moreover, we found no
132 difference in the fraction of drug-event pairs with significant ADE risk at child development
133 stages (Table 2; proportion test p-value=0.39). We found that the GAM identified two real-world
134 pediatric drug events with putative dynamic ADE risk (Figure 7). Specifically, the GAM showed
135 periods of lower risk during early and late childhood and higher risk during the middle stages of
136 childhood. While the PRR and GAM performed approximately the same overall, the GAM
137 captured dynamic ADE risk where the PRR did not.

138 **Discussion**

139 Children undergo a period of dynamic growth and development, presenting a challenge in
140 identifying and evaluating adverse drug events^{10,36}. We hypothesize that dynamic ontogenic
141 processes as children grow and develop may be reflected by temporal drug event reporting in the
142 population. We presented the first study to evaluate drug event reporting patterns across
143 childhood in large observational data. We found that GAMs, a population modeling technique,
144 outperformed the PRR, a population stratification method, as well as generated robust risk scores
145 to detect adverse drug events during childhood. This work represents a first step in transitioning
146 from performing event surveillance towards uncovering putative mechanisms of pediatric
147 adverse drug events.

148 The goal of our study is to improve the specificity of top-down data mining for generating
149 pediatric drug safety hypotheses. Our study hypothesis was temporal drug event reporting trends
150 found in observational data are dependent on ontogeny, which exhibits high and low molecular
151 and physiological levels throughout childhood^{7,37,38}. To test this within a top-down approach, we
152 generated temporal trends in observational data to correspond with temporal trends from
153 ontogeny as opposed to identifying temporal trends from frequency³⁹ or feature-derived^{40,41}
154 measures directly from observed data. This motivated both simulating dynamic drug event
155 reporting rates and then augmenting real-world data to generate different classes of dynamic
156 drug event reporting trends. While we simulated dynamic drug event reporting rates, we showed
157 that augmenting the FAERS data did not change the overall characteristics of the pediatric drug
158 reports. This was crucial for establishing the use of real-world drug event data to evaluate hidden
159 dynamic reporting trends. Importantly the ADE detection methods were in fact able to identify

160 the simulated dynamics within the data. The data simulation and augmentation of FAERS laid
161 the foundation for evaluating statistical methods to investigate ontogenic-mediated adverse event
162 mechanisms.

163 We found that the generalized additive model (GAM) showed improved detection of dynamic
164 drug event reporting compared to the proportional reporting ratio (PRR). While the PRR
165 produces ADE risk scores that were more erratic and unable to be computed, the GAM scores
166 were both more flexible and robust. The GAM assumes a flexible relationship yet reduces
167 ‘wiggleness’ to stable risk estimates based on observed data^{42,43}. While bayesian modeling
168 techniques such as Monte Carlo Markov Chain can also learn flexible relationships from
169 observed data, these models still require expert knowledge to build, implement, and interpret⁴⁴.
170 The GAM, on the other hand, generates an interpretable smooth relationship in a familiar
171 regression framework³² that shares information across child development stages. Using this
172 shared information framework, the GAM was able to detect injected dynamic ADE risks across
173 childhood even when drug event reporting was low. We further showed that the GAM not only
174 generated visually dynamic ADE risk when injecting dynamics, but we also identified putative
175 dynamic risk for real-world psychiatric adverse events from exposure to montelukast medication
176 (Figure S8). We demonstrated that GAMs can be used to detect dynamic reporting of adverse
177 drug events by sharing information across child development stages.

178 This study has some limitations. First, observational data has inherent bias and confounding
179 factors which may affect both the sample of drug-event pairs in our study as well as the
180 performance of the detection methods. We showed that the random sample of drug events
181 correspond to the reporting patterns found in the FAERS database. Also, performing a power
182 analysis allowed for identifying drug events for which the detection methods were able to

183 identify the dynamic reporting to provide a fair performance comparison. Second, other
184 regulatory agencies, such as the Food and Drug Administration and European Medicines
185 Agency, define pediatric age ranges for development stages by different methods. While varying
186 child stage definitions were not explored here, we chose stages defined by NICHD that were
187 established after consultation and agreement among several US-based organizations such as the
188 American Academy of Pediatrics and the Centers for Disease Control and Prevention⁴⁵. Third,
189 fixed development stages may serve more useful in drug regulations and trial design than
190 representing dynamic child growth and development. Nevertheless, the detection performance
191 and risk scores for both methods could only be compared when considering data found within
192 child development strata. Fortunately, the further advantage of the GAM is its ability to model
193 childhood as a continuous period using age without restrictive strata. This increases the sharing
194 of information for identifying adverse event risk during childhood which may cross development
195 stages and affect specific periods during childhood.

196 **Conclusion**

197 In this study, we evaluated ADE risk detection methods to identify dynamic drug event reporting
198 within observational data. By simulating drug event reporting and augmenting simulated rates
199 into existing observational data, we can make comparisons between methods to detect dynamic
200 drug event reporting patterns. We found GAMs result in more robust scores, overall improved
201 performance to detect dynamics, and improved ability to detect simulated and real-world
202 pediatric drug-events compared to the state-of-the-art PRR method. This study lays the
203 foundation to detect and evaluate pediatric adverse drug events for ontogenic-mediated
204 mechanisms.

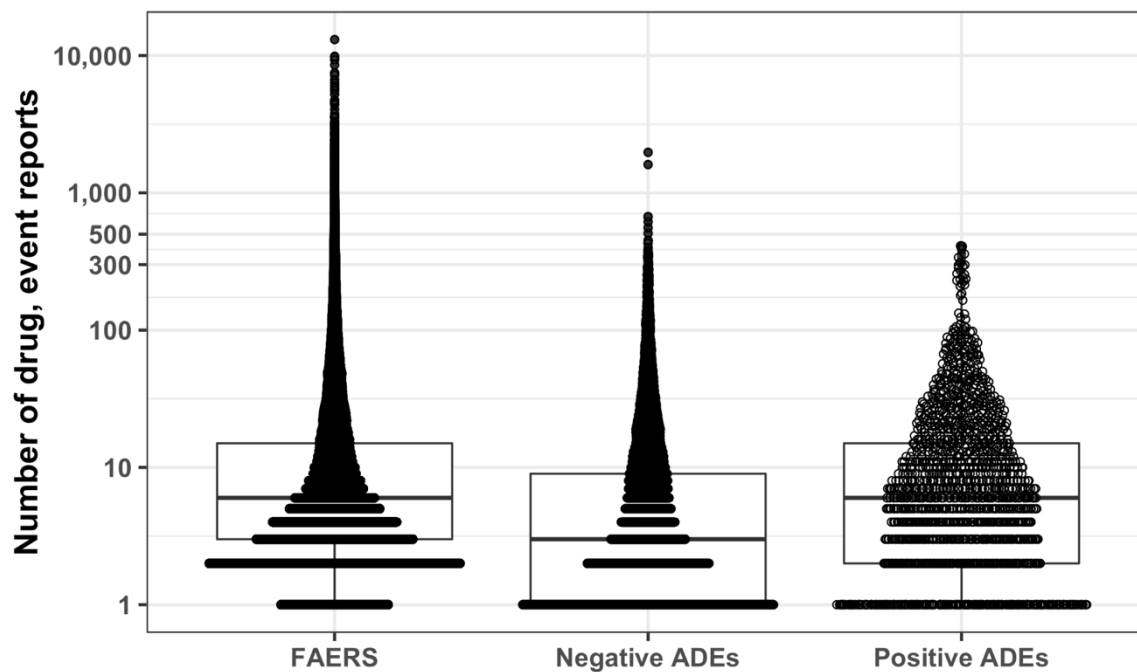


Fig. 1 Comparison of drug event reporting in drug-event datasets. A boxplot summary overlaid by the amount of drug event reports for drug-event pairs between (pediatric) FAERS (N=519,555), the positive control set (N=500), and the negative control set (N=10000). 'N' is the sample size.

205

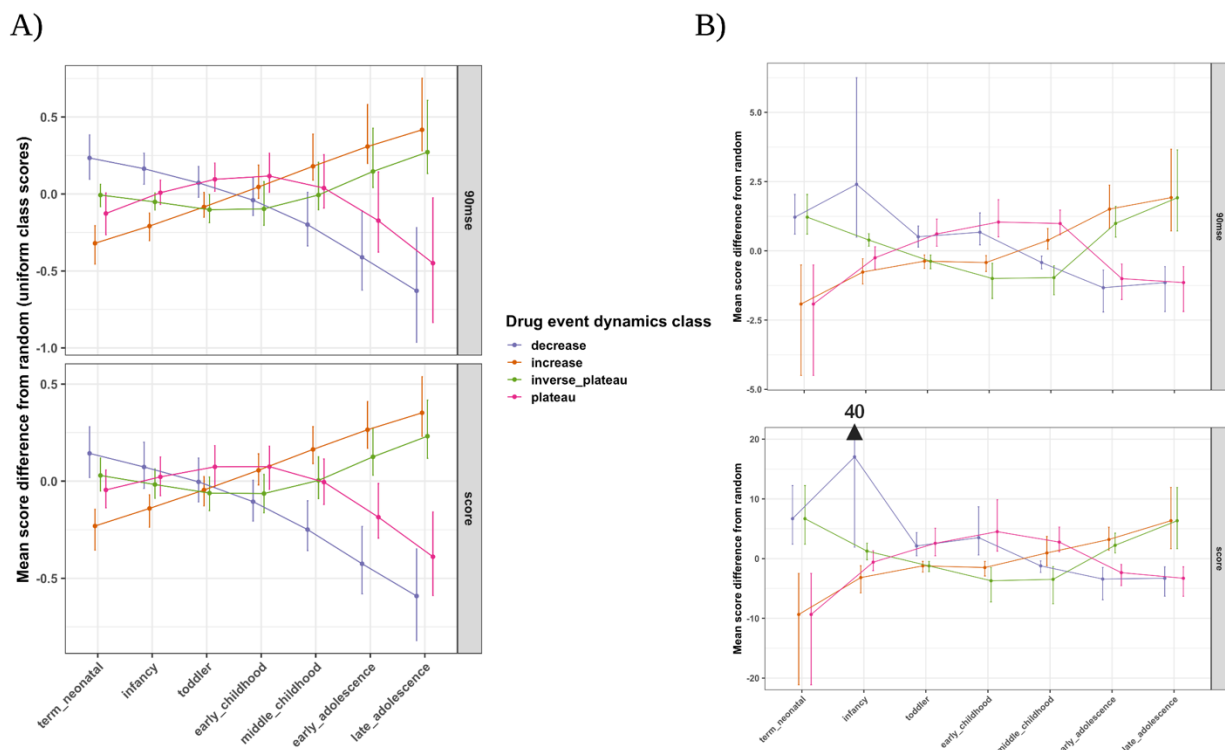


Fig. 2 ADE detection method risk score distribution across child development stages. Risk scores resulting from applying the A) GAM and B) PRR ADE detection methods on the positive control drug-event pair data for each dynamics class. The score distributions at each child development stage were produced after 100 bootstraps of the original scores for each method and score type. We show the average difference of the resampled score distributions between a given drug event reporting dynamics class and uniform (random drug event reporting across childhood) with the 95% confidence interval.

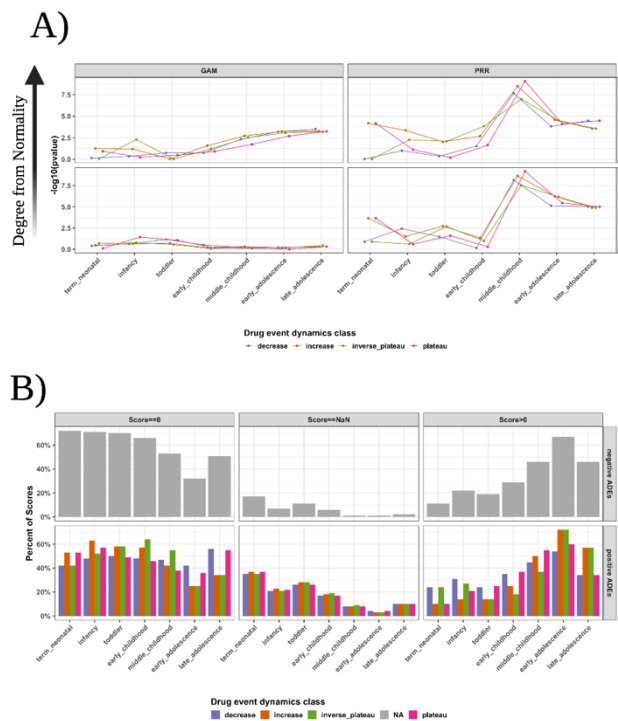


Fig. 3 Summary of ADE detection method risk score quality. A) Deviation from a normal score distribution for each method and score type across child development stages. The score distributions were produced after 100 bootstraps of the original scores at each child development stage. The Shapiro-Wilk test calculated a significance probability value for the resampled scores being drawn from a normal distribution. B) PRR detection method risk score quality summary. Across the positive and negative controls as well as drug event reporting dynamics classes, we calculated the number of scores with a zero, NaN (unable to be computed; the drug not reported at a stage or the drug not reported with the event at a stage), or nonzero positive score across child development stages.

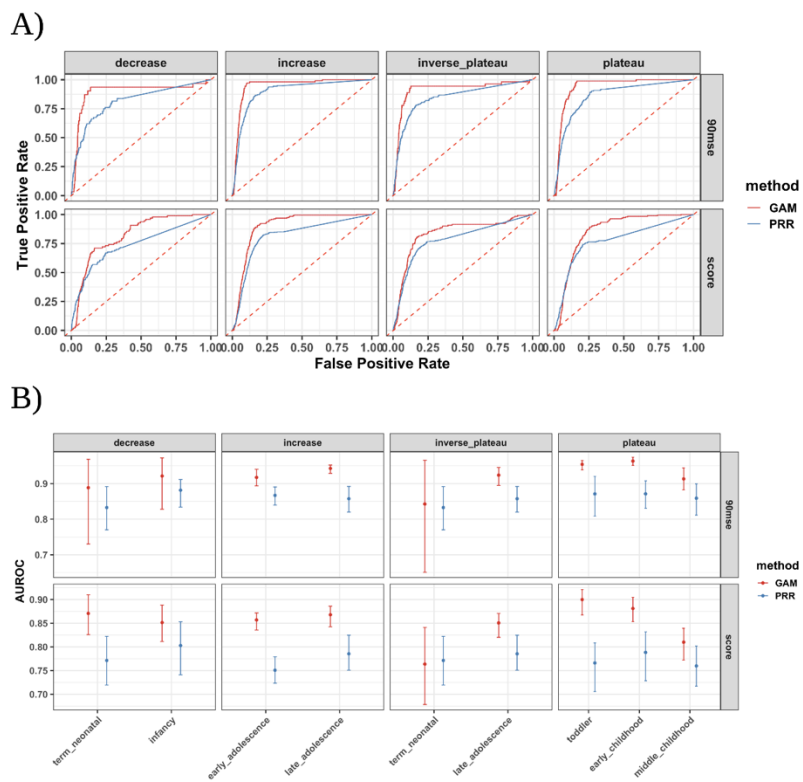


Fig. 4 GAM and PRR drug event dynamic detection performance. A) The receiver operating characteristic curves showing the true positive rate versus the false positive rate for each method and score type by drug event reporting dynamics class. B) The area under the receiver operating characteristic curve (AUROC) for each child development stage within each dynamics class.

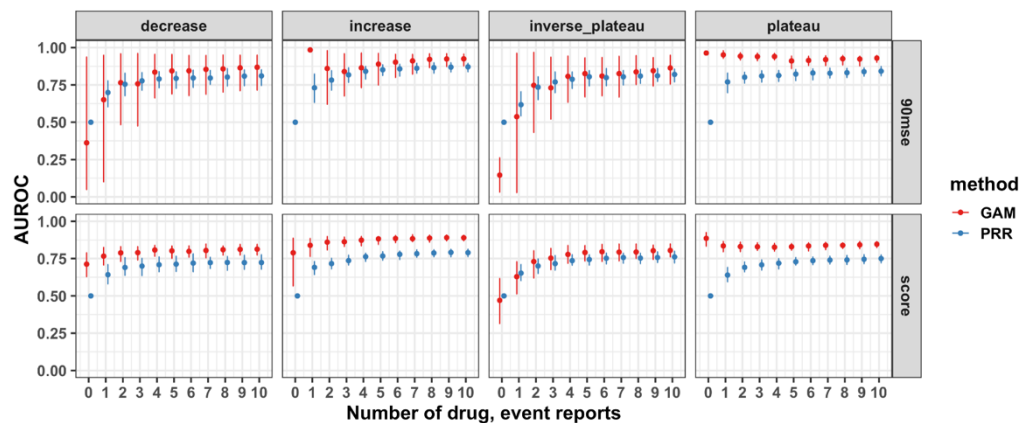


Fig. 5 GAM and PRR detection performance at low drug event reporting. The AUROC was computed for each method and score type to detect dynamics only utilizing (drug-event, stage, dynamic) triples with up to a given amount of drug event reports.

209

Table 1 Real-world pediatric drug-event detection performance. The area under the receiver operating characteristic curve (AUROC) and sensitivity or true positive rate to detect real-world pediatric drug-events observed within FAERS per each method and score type. The prediction threshold for the sensitivity was the null statistic for each method (null threshold: GAM==0; PRR==1). The performance interval is the 95% confidence interval.

| | Real-world pediatric drug-event detection performance | | | | | | | |
|-------------------|---|----------------------|----------------------|----------------------|----------------------|----------------------|----------------------|----------------------|
| | AUROC | | | | Sensitivity | | | |
| | 90mse | | score | | 90mse | | score | |
| | PRR | GAM | PRR | GAM | PRR | GAM | PRR | GAM |
| Performance value | 0.62 [0.58, 0.66] | 0.65 [0.59, 0.69] | 0.62 [0.58, 0.67] | 0.73 [0.69, 0.77] | 0.28 [0.22, 0.36] | 0.28 [0.23, 0.35] | 0.49 [0.40, 0.56] | 0.85 [0.81, 0.89] |

210

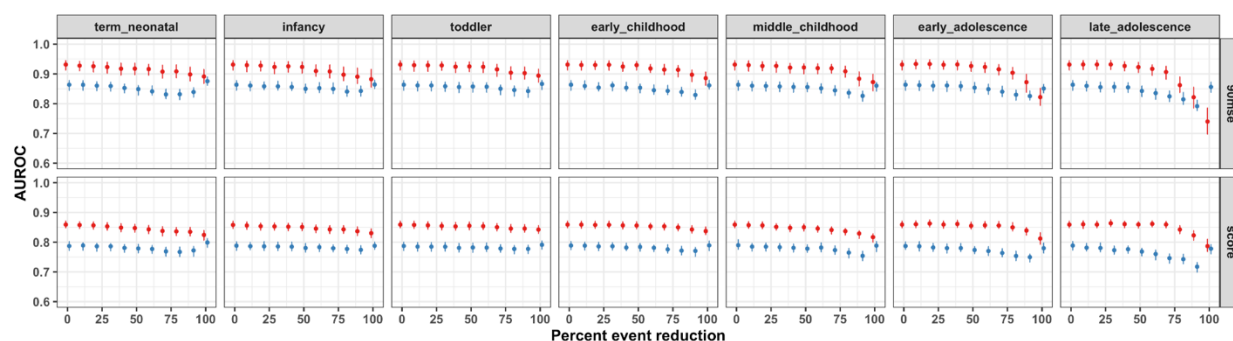


Fig. 6 GAM and PRR performance to detect dynamic patterns of rare adverse events. The AUROC for detecting various classes of drug event reporting dynamics as event reporting was reduced at child development stages. The event reporting for drug-event pairs was reduced at 10% decrements only within a specific child development stage. For example, 0% event reporting reduction indicates no reduction in event reporting and 100% event reporting reduction indicates all event reports were removed.

211

Table 2 ADE detection method risk score quality and significance on real-world pediatric drug-events. The number of drug-event pairs that contained a child development stage with a risk score of each score quality (null threshold: GAM==0; PRR==1). A 90% lower bound score above the null threshold indicates a significant risk.

| Number of drug-event pairs with score quality in at least one stage | Zero | NaN | Finite | Infinite | Score above null | 90% lower bound above null |
|---|------|-----|--------|----------|------------------|----------------------------|
| GAM | 0 | 0 | 26 | 0 | 26 | 14 |
| PRR | 23 | 14 | 25 | 5 | 26 | 18 |

212

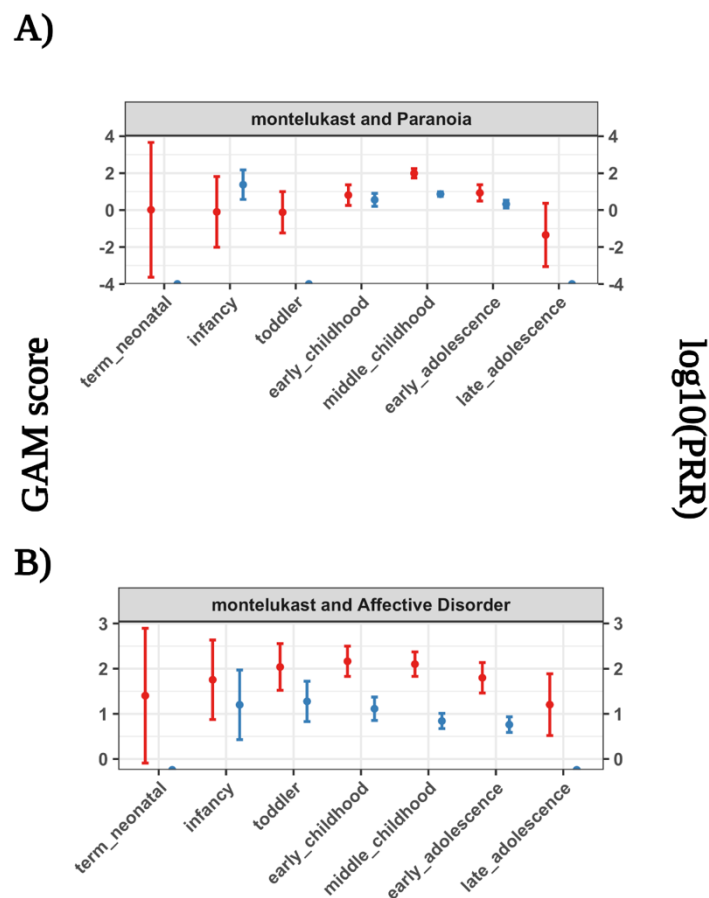


Fig. 7 GAM and PRR detection scores on putative real-world dynamic adverse drug events. We highlight two psychiatric adverse events, A) Paranoia and B) Affective Disorder, from exposure to the drug montelukast exhibiting dynamic ADE risks across child development stages.

213

214 **Methods**

215 *ADE data source*

216 We retrieved drug event reports from the Food and Drug Administration's openFDA⁴⁶ download

217 page, utilizing an API key with extended permissions, containing the FAERS data. Using custom

218 python notebooks and scripts available in the ‘openFDA_drug_event-parsing’ github repository
219 (DOI: 10.5281/zenodo.4464544), we extracted and formatted all drug event reports prior to the
220 third quarter of 2019. Data fields included the safety report identifier, age value, age code
221 e.g. year, adverse event MedDRA concept code (preferred terms), and drug RxNorm code
222 (various) used in our analyses. The age value was standardized to year units for categorizing
223 reports into the 7 child development stages according to the Eunice Kennedy Shriver National
224 Institute of Child and Human Development⁴⁵. Adverse drug event MedDRA codes were mapped
225 to standard concept identifiers using concept tables⁴⁸ from the OMOP common data model. The
226 drug RxNorm code was similarly translated to the standard RxNorm concept identifier
227 (ingredient level) in OMOP and was further mapped to the equivalent ATC concept identifier
228 (ATC 5th level) using the concept relationship table. The occurrence of an adverse drug event is
229 defined as any safety report where both the adverse event and drug concepts are reported
230 together. The pediatric report space for any adverse drug event is all reports which have age
231 above zero and less than or equal to 21 years old which is the upper bound for the late
232 adolescence child development stage. The drug event data for a given drug-event pair composed
233 of 339,741 safety reports with a binary indicator for reports of the event and drug, as well as the
234 category of NICHD child development stage for the report’s patient.

235 *Simulated ADE dynamics*

236 The objective of this study was to evaluate detection of drug-event reporting as the reporting rate
237 changes across child development stages with varying dynamics and effect sizes. We assert that
238 reporting dynamics during childhood reflect ontogenic profiles observed on molecular,
239 functional, and structural levels^{7,37,38}.

240 We simulated dynamic ADE reporting by combining hyperbolic tangent functions that produced
241 symmetric probability distributions around a given effect size to define the probability of event
242 reporting at drug reports. These dynamic reporting classes represent nonlinear trends of drug-
243 event reports across childhood. The average drug and event reporting across reports equaled the
244 event reporting rate multiplied by a fold change factor resulting in the effect size of dynamic
245 drug event reporting. The fold change followed a negative exponential distribution with rate
246 parameter 0.75 resulting in a fold change distribution ranging from 1 to 10 (Figure S9). The
247 simulated reporting probabilities were distributed to safety reports in age ascending order
248 reflecting a desired dynamic distribution of ADE reporting across childhood. We designed 5
249 different dynamic reporting rates, namely ‘uniform’ (random), ‘increase’, ‘decrease’, ‘plateau’,
250 and ‘inverse_plateau’ (Figure S10).

251 *ADE data augmentation*

252 We augmented the original drug event data from FAERS with the simulated drug event reporting
253 dynamics. We randomly selected 500 drug-event pairs to be the positive control set. We
254 augmented the drug event data for each pair with dynamics previously described that we want to
255 detect. We then randomly selected 10,000 mutually exclusive drug-event pairs to be the negative
256 control set which were not augmented and represented reporting of drugs with events within
257 FAERS. Differences of the average drug event reporting between the drug-event sets was
258 computed by comparing 10 million resamples of each distribution.

259

260 Augmenting the positive control drug-event pairs resulted in 5 sets of 500 drug-event pairs,
261 forming (drug-event, stage, dynamic) triples. The (drug-event, stage, uniform dynamic) triple

262 scores were the reference distribution for comparing the average difference in scores, after 20
263 resamples, with ADE risk scores from the other dynamics classes.

264 *ADE detection methods*

265 We applied two ADE detection methods to the positive and negative control drug-event sets. We
266 chose a population stratification (PRR) and modeling (GAM) method to evaluate detection of
267 ADE dynamics when stratifying the data or by sharing information across child development
268 stages, respectively.

269 We employed the Proportional Reporting Ratio (PRR):

$$270 \quad \frac{\frac{a}{a+c}}{\frac{b}{b+d}}$$

271 where ‘a’ is the number of reports with the drug and event, ‘b’ is the number of reports without
272 the drug and with the event, ‘c’ is the number of reports with the drug and without the event, and
273 ‘d’ is the number of reports without the drug or event of interest. The resulting score is the event
274 reporting prevalence with the drug compared to without the drug. We generated PRR scores for
275 each child development stage resulting in 7 scores for each drug-event pair. The PRR scores
276 were log₁₀ transformed when conducting the Shapiro-Wilk test for normality.

277 We also evaluated the logistic generalized additive model⁴⁹ (GAMs):

$$278 \quad g(E(Event)) = s(nichd) * Drug$$

279 where g is a logit link function, $E(Event)$ is the expected value of event reporting, s is a spline
280 function with a penalized cubic basis, $nichd$ is the child development stage of the report’s

281 subject, and *Drug* is an indicator i.e. 0 or 1 of drug reporting. Details for GAMs can be found at
282 references^{42,50} and we specified the model using the *mgcv* package in R.

283 Briefly, the GAM is a flexible statistical model that captures nonlinear effects of covariates onto
284 a response. In this paper, we model the effect of the child development stage interacting with
285 drug reporting on the reporting of an event where the event is the reporting of the MedDRA
286 preferred term and the drug is the reporting of the ATC 5th level drug concept. The *s()* function
287 is a spline function where the interaction of the child development stage (main effect) and the
288 drug (interaction using the ‘by’ variable) is modeled according to a set of basis functions. Each
289 development stage defines the knot (7 in total) in which the expectation of event reporting is
290 quantified. In the spline function, a penalized cubic spline basis (bs=‘cs’) is used for fitting the
291 basis functions where the first and second derivative of the event expectation is zero at each
292 knot, resulting in a smooth event expectation across stages. To mitigate overfitting or
293 ‘wiggleness’, we used a penalized iterative restricted likelihood approach, called ‘fREML’, with
294 a wiggleness penalty in the objective function. Fitting the GAM model (using the ‘bam’ function
295 and discrete=T) produces coefficient terms, similar to beta coefficients in logistic regression, for
296 each child development stage for the association of the adverse event being reported in
297 interaction with reporting the drug. We generated GAM scores for each child development stage
298 resulting in 7 scores for each drug-event pair. It is important to note that all GAM scores
299 produced were finite, nonzero values.

300 The scores generated by each method have different variations and uncertainty in the estimated
301 population value. We additionally determined the lower confidence bound in which the
302 population-based score would be greater than 90% of score replicates. The population score and

303 the 90% lower confidence bound, called ‘score’ and ‘90mse’ respectively, are the score types for
304 each method.

305 *ADE dynamic detection power analysis*

306 We performed a power analysis to determine which of the positive control drug-event pairs could
307 be detected for each method and score type. The generated scores may not show a drug and event
308 association (score above the null statistic or a significance association) for a child development
309 stage due to the method’s different assumptions and biases when applied onto observational data.
310 To mitigate these issues, we determined the drug event data characteristics, namely the number
311 of drug reports and the effect size, for each method in which reporting dynamics could be
312 detected at or above $t = 80\%$ power or true positive rate. Specifically, for the (drug-event, stage,
313 dynamic) triple scores in the positive control set, we determined the power to differentiate scores
314 at high reporting rates about a given score threshold (GAM score threshold==0; PRR score
315 threshold==1). The reporting rates were higher at different child development stages for each
316 dynamics class e.g. the ‘increase’ dynamics class had higher reporting at the ‘early_adolescence’
317 and ‘late_adolescence’ stages (Table S1). The scores from (drug-event, stage, dynamic) triples
318 with a high reporting rate were only considered for reflecting dynamic drug event reporting
319 associations. The scores from (drug-event, stage, dynamic) triples with a low reporting rate were
320 not considered further due to spurious scores generated at stages without injected signal. The
321 drug event characteristics were determined for both the estimated population score (‘score’) and
322 the 90% lower bound score (‘90mse’) that represent scores with lower and higher confidence,
323 respectively, for the ‘true’ population score.

324 Choosing drug-event pairs at or exceeding the characteristics for each method and score type at
325 or above $t = 80\%$ power resulted in a superset of (drug-event, stage, dynamic) triples designated
326 as positives in a reference standard for each drug event reporting dynamics class (Table S2). The
327 negative control set contained the same (drug-event, stage) doubles or 70,000 scores for each
328 reference standard. Excluding the drug-event scores generated by the uniform class, there were 4
329 reference standards of positive and negative drug-event pairs for each ADE reporting dynamics
330 class used for detection performance evaluation.

331 *ADE dynamic detection performance*

332 We evaluated the GAM and PRR methods to detect drug event reporting dynamics across the
333 child development stages. Specifically, we determined the performance in differentiating scores
334 from (drug-event, stage, dynamic) triples in the positive control set versus the negative control
335 (drug-event, stage) score doubles. The positive control set contained a superset of the 500 (drug-
336 event, stage, dynamic) score triples (Table S2). The negative control set contained the same
337 (drug-event, stage) doubles or 70,000 scores for each reference standard. For each of the four
338 reference standards, we quantified performance metrics including the sensitivity, specificity, and
339 area under the receiver operating characteristic (AUROC) curve using the R package *ROCR* for
340 each detection method and score type. Confidence intervals for the AUROC were calculated
341 through bootstrapping (100 resamples) the score distributions and calculating performance
342 metric values.

343 *Dynamics sensitivity analysis*

344 We assessed the sensitivity of the ADE detection methods to detect drug event reporting
345 dynamics within child development stages. We artificially reduced, at 10% decrements, the event

346 reporting rate at each child development stage separately. Specifically, at each reduced stage, we
347 determined the sensitivity of each method and score type to detect (drug-event, stage, dynamic)
348 score triples compared to the same negative control (drug-event, stage) score doubles at that
349 same reduced stage. Sensitivity was assessed iteratively at the 10% decrements within each child
350 development stage. We calculated the AUROC and power metrics to quantify sensitivity to drug
351 event reporting dynamics for each method and score type.

352 *Real-world ADE validation*

353 We applied the ADE detection methods on observed FAERS data for drug-event pairs within the
354 pediatric drug-event reference standard from the Global Research in Pediatrics consortium⁵¹. A
355 machine-readable dataset can be found at the ‘GRiP_pediatric_ADE-reference_set’ github
356 repository (DOI: 10.5281/zenodo.4453379). We assigned drug-event pairs with epidemiological
357 or mechanistic evidence in children (Control==‘C’) as the positive class (N=26), and the cross-
358 product of all drugs and events that were complementary to drug-event pairs in the reference set
359 as the negative class (N=123). We calculated the AUROC using the *ROCR* package in R and the
360 true positive rate using the null statistic of each method as the prediction threshold.

361 **List of Abbreviations**

362 ADE: adverse drug event; FAERS: Food and Drug Administration Adverse Event Reporting
363 System; GAM: generalized additive model; PRR: proportional reporting ratio; NICHD: national
364 institute of child and human development; AUROC: area under the receiver operating
365 characteristic curve; TPR: true positive rate; ATC: anatomical therapeutic class; DOI: digital
366 object identifier.

367 **Availability of Data and Materials**

368 The datasets and code supporting the conclusions of this article are available in the
369 ‘evaluating_ontogenic_ade_risk’ Github repository, DOI: 10.5281/zenodo.4585585.

370

371 **Declarations**

372 None.

373 **References**

- 374 1. Impicciatore P, Choonara I, Clarkson A, Provasi D, Pandolfini C, Bonati M. Incidence of
375 adverse drug reactions in paediatric in/out-patients: a systematic review and meta-analysis
376 of prospective studies. *Br J Clin Pharmacol*. 2001;52(1):77-83. doi:10.1046/j.0306-
377 5251.2001.01407.x
- 378 2. Smyth RMD, Gargon E, Kirkham J, et al. Adverse drug reactions in children--a systematic
379 review. *PLoS One*. 2012;7(3):e24061. doi:10.1371/journal.pone.0024061
- 380 3. Giangreco NP, Elias JE, Tatonetti NP. No population left behind: Improving paediatric
381 drug safety using informatics and systems biology. *Br J Clin Pharmacol*. Published online
382 December 17, 2020:bcp.14705. doi:10.1111/bcp.14705
- 383 4. Benjamin DK, Smith PB, Sun MJM, et al. Safety and Transparency of Pediatric Drug
384 Trials. *Arch Pediatr Adolesc Med*. 2009;163(12):1080-1086.
385 doi:10.1001/archpediatrics.2009.229

- 386 5. de Bie S, Ferrajolo C, Straus SMJM, et al. Pediatric Drug Safety Surveillance in FDA-
387 AERS: A Description of Adverse Events from GRiP Project. Garattini S, ed. *PLoS One*.
388 2015;10(6):e0130399. doi:10.1371/journal.pone.0130399
- 389 6. Castro-Pastrana LI, Carleton BC. Improving pediatric drug safety: need for more efficient
390 clinical translation of pharmacovigilance knowledge. *J Popul Ther Clin Pharmacol = J la*
391 *Ther des Popul la Pharmacol Clin*. 2011;18(2):e76-88.
392 <http://journals.sagepub.com/doi/10.1038/jcbfm.2012.176>
- 393 7. Crespi B. The evolutionary biology of child health. *Proc R Soc B Biol Sci*.
394 2011;278(1711):1441-1449. doi:10.1098/rspb.2010.2627
- 395 8. Yaffe S, Estabrook RW, Pitluck S, Davis JR. *Rational Therapeutics for Infants and*
396 *Children.*; 2000. doi:10.17226/9816
- 397 9. Johnson T. The development of drug metabolising enzymes and their influence on the
398 susceptibility to adverse drug reactions in children. *Toxicology*. 2003;192(1):37-48.
399 doi:10.1016/S0300-483X(03)00249-X
- 400 10. Becker ML, Leeder JS. Identifying genomic and developmental causes of adverse drug
401 reactions in children. *Pharmacogenomics*. 2010;11(11):1591-1602.
402 doi:10.2217/pgs.10.146
- 403 11. de Graaf-Peters VB, Hadders-Algra M. Ontogeny of the human central nervous system:
404 What is happening when? *Early Hum Dev*. 2006;82(4):257-266.
405 doi:10.1016/j.earlhumdev.2005.10.013
- 406 12. Simon AK, Hollander GA, McMichael A. Evolution of the immune system in humans

- 407 from infancy to old age. *Proceedings Biol Sci.* 2015;282(1821):20143085.
408 doi:10.1098/rspb.2014.3085
- 409 13. Carvalho FS, Burgeiro A, Garcia R, Moreno AJ, Carvalho RA, Oliveira PJ. Doxorubicin-
410 Induced Cardiotoxicity: From Bioenergetic Failure and Cell Death to Cardiomyopathy.
411 *Med Res Rev.* 2014;34(1):106-135. doi:10.1002/med.21280
- 412 14. Guo H-L, Jing X, Sun J-Y, et al. Valproic Acid and the Liver Injury in Patients with
413 Epilepsy: An Update. *Curr Pharm Des.* 2019;25(3):343-351.
414 doi:10.2174/1381612825666190329145428
- 415 15. Moon YE. Paradoxical reaction to midazolam in children. *Korean J Anesthesiol.*
416 2013;65(1):2-3. doi:10.4097/kjae.2013.65.1.2
- 417 16. Kawakami Y, Fujii S, Ishikawa G, Sekiguchi A, Nakai A, Takase M. Valproate-induced
418 polycystic ovary syndrome in a girl with epilepsy: A case study. *J Nippon Med Sch.*
419 2018;85(5):287-290. doi:10.1272/jnms.JNMS.2018_85-46
- 420 17. Cui N, Wu F, Lu W, et al. Doxorubicin-induced cardiotoxicity is maturation dependent
421 due to the shift from topoisomerase II α to II β in human stem cell derived cardiomyocytes.
422 *N.* 2019;23(7):4627-4639. doi:10.1111/jcmm.14346
- 423 18. Park SO, Wamsley HL, Bae K, et al. Conditional Deletion of Jak2 Reveals an Essential
424 Role in Hematopoiesis throughout Mouse Ontogeny: Implications for Jak2 Inhibition in
425 Humans. *PLoS One.* 2013;8(3):1-14. doi:10.1371/journal.pone.0059675
- 426 19. Marret S, Mukendi R, Gadiuseux JF, Gressens P, Evrard P. Effect of ibotenate on brain
427 development: An excitotoxic mouse model of microgyria and posthypoxic-like lesions. *J*

- 428 *Neuropathol Exp Neurol.* 1995;54(3):358-370. doi:10.1097/00005072-199505000-00009
- 429 20. Jiang X-L, Zhao P, Barrett J, Lesko L, Schmidt S. Application of Physiologically Based
430 Pharmacokinetic Modeling to Predict Acetaminophen Metabolism and Pharmacokinetics
431 in Children. *CPT Pharmacometrics Syst Pharmacol.* 2013;2(10):80.
432 doi:10.1038/psp.2013.55
- 433 21. Krekels EHJ, Neely M, Panoilia E, et al. From pediatric covariate model to
434 semiphysiological function for maturation: Part I-extrapolation of a covariate model from
435 morphine to zidovudine. *CPT Pharmacometrics Syst Pharmacol.* 2012;1(1):1-8.
436 doi:10.1038/psp.2012.11
- 437 22. Baldrick P. Juvenile animal testing in drug development - Is it useful? *Regul Toxicol*
438 *Pharmacol.* 2010;57(2-3):291-299. doi:10.1016/j.yrtph.2010.03.009
- 439 23. Goulooze SC, Zwep LB, Vogt JE, et al. Beyond the Randomized Clinical Trial:
440 Innovative Data Science to Close the Pediatric Evidence Gap. *Clin Pharmacol Ther.*
441 2020;107(4):786-795. doi:10.1002/cpt.1744
- 442 24. Brussee JM, Calvier EAM, Krekels EHJ, et al. Children in clinical trials: towards
443 evidence-based pediatric pharmacotherapy using pharmacokinetic-pharmacodynamic
444 modeling. *Expert Rev Clin Pharmacol.* 2016;9(9):1235-1244.
445 doi:10.1080/17512433.2016.1198256
- 446 25. Christensen ML, Davis RL. Identifying the “Blip on the Radar Screen”: Leveraging Big
447 Data in Defining Drug Safety and Efficacy in Pediatric Practice. *J Clin Pharmacol.*
448 2018;58(January):S86-S93. doi:10.1002/jcph.1141

- 449 26. Tatonetti NP. Translational medicine in the Age of Big Data. *Brief Bioinform.*
450 2019;20(2):457-462. doi:10.1093/bib/bbx116
- 451 27. Berlin JA, Glasser SC, Ellenberg SS. Adverse event detection in drug development:
452 Recommendations and obligations beyond phase 3. *Am J Public Health.* 2008;98(8):1366-
453 1371. doi:10.2105/AJPH.2007.124537
- 454 28. Etwel FA, Rieder MJ, Bend JR, Koren G. A Surveillance Method for the Early
455 Identification of Idiosyncratic Adverse Drug Reactions. *Drug Saf.* 2008;31(2):169-180.
456 doi:10.2165/00002018-200831020-00006
- 457 29. Star K, Sandberg L, Bergvall T, Choonara I, Caduff-Janosa P, Edwards IR. Paediatric
458 safety signals identified in Vigibase: Methods and results from Uppsala Monitoring
459 Centre. *Pharmacoepidemiol Drug Saf.* 2019;28(5):680-689. doi:10.1002/pds.4734
- 460 30. Evans SJW, Waller PC, Davis S. Use of proportional reporting ratios (PRRs) for signal
461 generation from spontaneous adverse drug reaction reports. *Pharmacoepidemiol Drug Saf.*
462 2001;10(6):483-486. doi:10.1002/pds.677
- 463 31. Osokogu OU, Dodd C, Pacurariu A, Kaguelidou F, Weibel D, Sturkenboom MCJM. Drug
464 Safety Monitoring in Children: Performance of Signal Detection Algorithms and Impact
465 of Age Stratification. *Drug Saf.* 2016;39(9):873-881. doi:10.1007/s40264-016-0433-x
- 466 32. Hastie T, Tibshirani R, Friedman J. *Elements of Statistical Learning*. 2nd editio. Springer;
467 2008. <http://web.stanford.edu/~hastie/pub.htm>
- 468 33. Guisan A, Edwards TC, Hastie T. Generalized linear and generalized additive models in
469 studies of species distributions: setting the scene. *Ecol Modell.* 2002;157(2-3):89-100.

470 doi:10.1016/S0304-3800(02)00204-1

471 34. Yin Q, Wang J. The association between consecutive days' heat wave and cardiovascular
472 disease mortality in Beijing, China. *BMC Public Health*. 2017;17(1):1-10.

473 doi:10.1186/s12889-017-4129-7

474 35. Tamayo-Uria I, Mateu J, Escobar F, Mughini-Gras L. Risk factors and spatial distribution
475 of urban rat infestations. *J Pest Sci (2004)*. 2014;87(1):107-115. doi:10.1007/s10340-013-

476 0530-x

477 36. Fabiano V, Mameli C, Zuccotti GV. Adverse drug reactions in newborns, infants and
478 toddlers: pediatric pharmacovigilance between present and future. *Expert Opin Drug Saf*.

479 2012;11(1):95-105. doi:10.1517/14740338.2011.584531

480 37. Saghir SA, Khan SA, McCoy AT. Ontogeny of mammalian metabolizing enzymes in
481 humans and animals used in toxicological studies. *Crit Rev Toxicol*. 2012;42(5):323-357.

482 doi:10.3109/10408444.2012.674100

483 38. Gunewardena SS, Yoo B, Peng L, et al. Deciphering the Developmental Dynamics of the
484 Mouse Liver Transcriptome. Buratti E, ed. *PLoS One*. 2015;10(10):e0141220.

485 doi:10.1371/journal.pone.0141220

486 39. Bohn J, Kortepeter C, Muñoz M, Simms K, Montenegro S, Dal Pan G. Patterns in
487 spontaneous adverse event reporting among branded and generic antiepileptic drugs. *Clin*

488 *Pharmacol Ther*. 2015;97(5):508-517. doi:10.1002/cpt.81

489 40. Bagattini F, Karlsson I, Rebane J, Papapetrou P. A classification framework for exploiting
490 sparse multi-variate temporal features with application to adverse drug event detection in

- 491 medical records. *BMC Med Inform Decis Mak.* 2019;19(1):1-21. doi:10.1186/s12911-018-
492 0717-4
- 493 41. Zhao J, Papapetrou P, Asker L, Boström H. Learning from heterogeneous temporal data in
494 electronic health records. *J Biomed Inform.* 2017;65:105-119.
495 doi:10.1016/j.jbi.2016.11.006
- 496 42. Wood SN. *Generalized Additive Models: An Introduction with R, Second Edition.*; 2017.
497 doi:10.1201/9781315370279
- 498 43. Helwig NE. Regression with ordered predictors via ordinal smoothing splines. *Front Appl*
499 *Math Stat.* 2017;3(July):1-13. doi:10.3389/fams.2017.00015
- 500 44. Simpson D, Rue H, Riebler A, Martins TG, Sørbye SH. Penalising model component
501 complexity: A principled, practical approach to constructing priors. *Stat Sci.* 2017;32(1):1-
502 28. doi:10.1214/16-STS576
- 503 45. Williams K, Thomson D, Seto I, et al. Standard 6: Age groups for pediatric trials.
504 *Pediatrics.* 2012;129(SUPPL. 3):S153-S160. doi:10.1542/peds.2012-0055I
- 505 46. Kass-Hout TA, Xu Z, Mohebbi M, et al. OpenFDA: An innovative platform providing
506 access to a wealth of FDA's publicly available data. *J Am Med Informatics Assoc.*
507 2016;23(3):596-600. doi:10.1093/jamia/ocv153
- 508 47. Giangreco NP. [ngiangre/openFDA_drug_event_parsing](https://github.com/ngiangre/openFDA_drug_event_parsing): Repository for python notebooks
509 and scripts for parsing the json-formatted drug event reports collected by the FDA.
510 Published online 2021. doi:<https://zenodo.org/badge/latestdoi/246321623>
- 511 48. OHDSI. Athena. Accessed January 17, 2021. <https://athena.ohdsi.org/search-terms/start>

- 512 49. Buja BYA, Hastie T, Tibshirani R. Linear Smoothers and Additive Models.
513 2016;17(2):453-510.
514 https://scholar.google.com/scholar_lookup?journal=The+Annals+of+Statistics&title=Line
515 [ar+smoothers+and+additive+models&author=A+Buja&author=T+Hastie&author=R+Tibs](https://scholar.google.com/scholar_lookup?journal=The+Annals+of+Statistics&title=Line)
516 [hirani&publication_year=1989&pages=453-510&](https://scholar.google.com/scholar_lookup?journal=The+Annals+of+Statistics&title=Line)
- 517 50. Hastie T, Tibshirani R. Generalized additive models for medical research. *Stat Methods*
518 *Med Res.* 1995;4(3):187-196. doi:10.1177/096228029500400302
- 519 51. Osokogu OU, Fregonese F, Ferrajolo C, et al. Pediatric drug safety signal detection: a new
520 drug-event reference set for performance testing of data-mining methods and systems.
521 *Drug Saf.* 2015;38(2):207-217. doi:10.1007/s40264-015-0265-0
- 522 52. Giangreco N. GRiP_pediatric_ADE-reference_set. Published 2020. Accessed October 21,
523 2020. https://github.com/ngiangre/GRiP_pediatric_ADE-reference_set
- 524 53. Giangreco NP. [ngiangre/evaluating_ontogenic_ade_risk](https://github.com/ngiangre/evaluating_ontogenic_ade_risk). Published online 2021.
525 doi:10.5281/zenodo.4585585

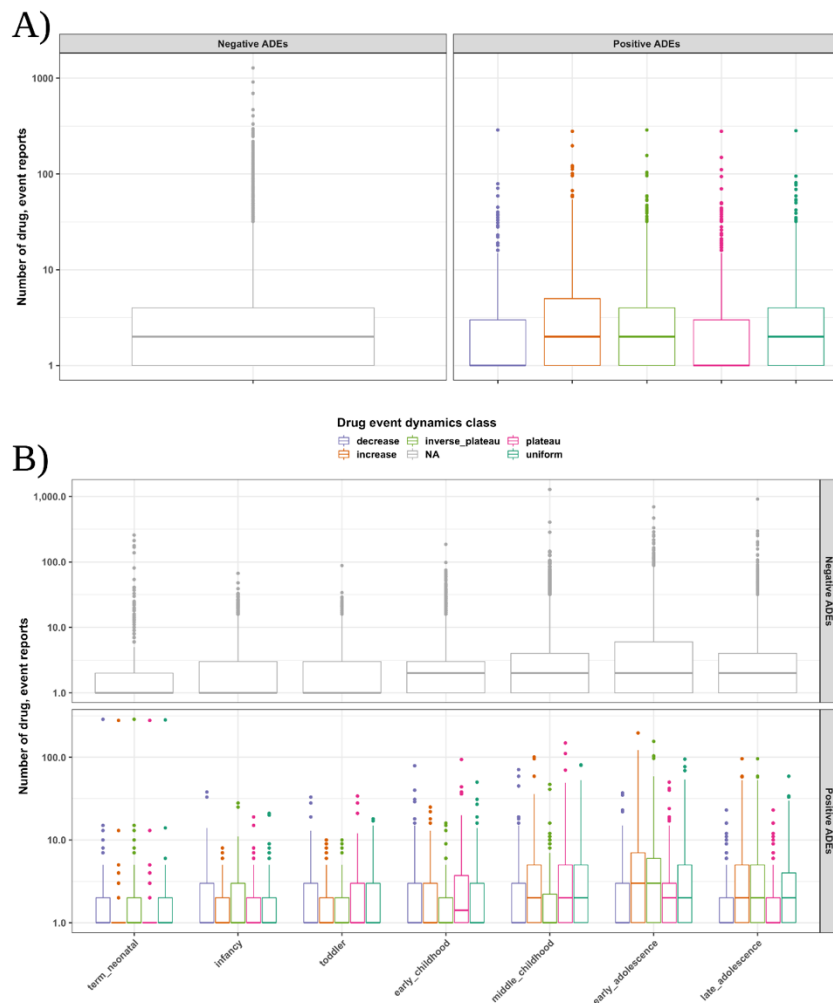


Fig. S1 Drug event reporting for positive and negative controls. The distribution of drug-event reporting between positive and negative control set drug-event pairs across A) dynamics classes and B) child development stages.

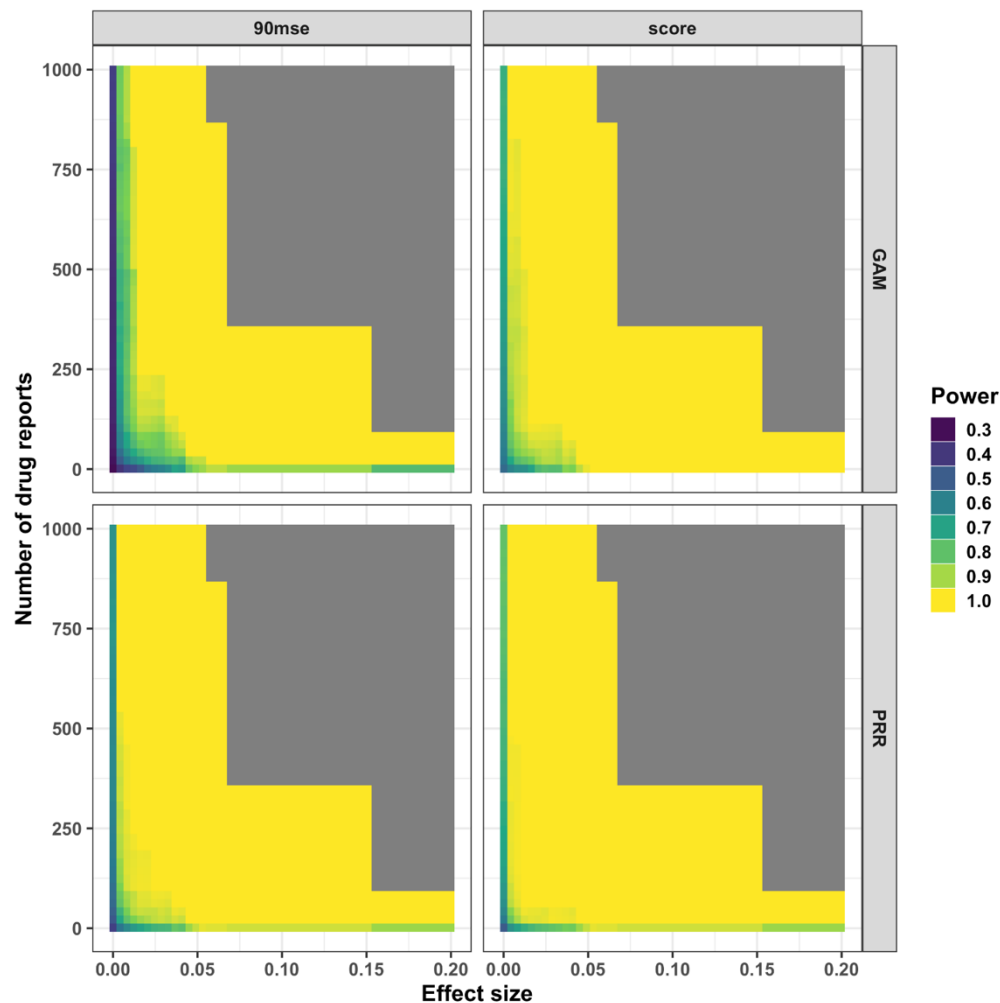


Fig. S2 Power graph detecting drug-event pairs with dynamics for each method and score type. The number of drug reports and effect size determined the scores evaluated to detect an association between the drug and event co-occurrence. The scores used were from child development stages with a high reporting rate determined by the dynamic class.

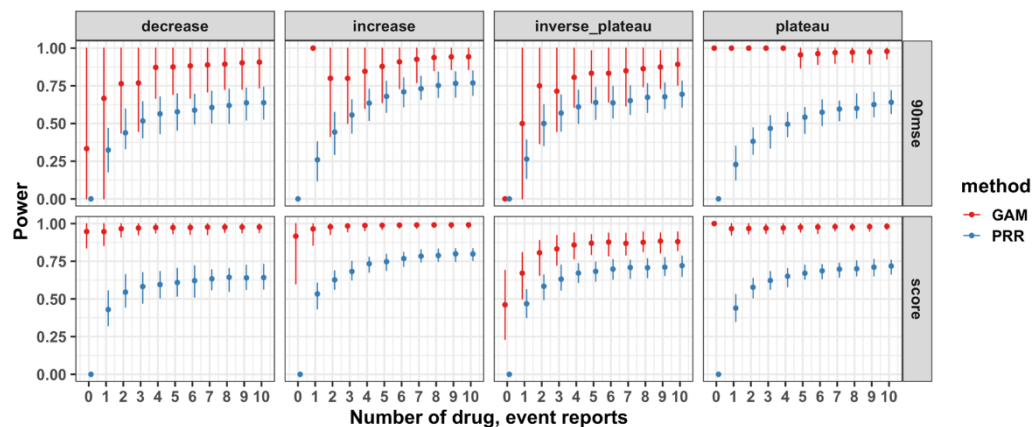


Fig. S3 GAM and PRR detection sensitivity at low drug event reporting. The sensitivity or true positive rate was computed for each method and score type to detect dynamics only utilizing (drug-event, stage, dynamic) triples with a given amount of drug event reports.

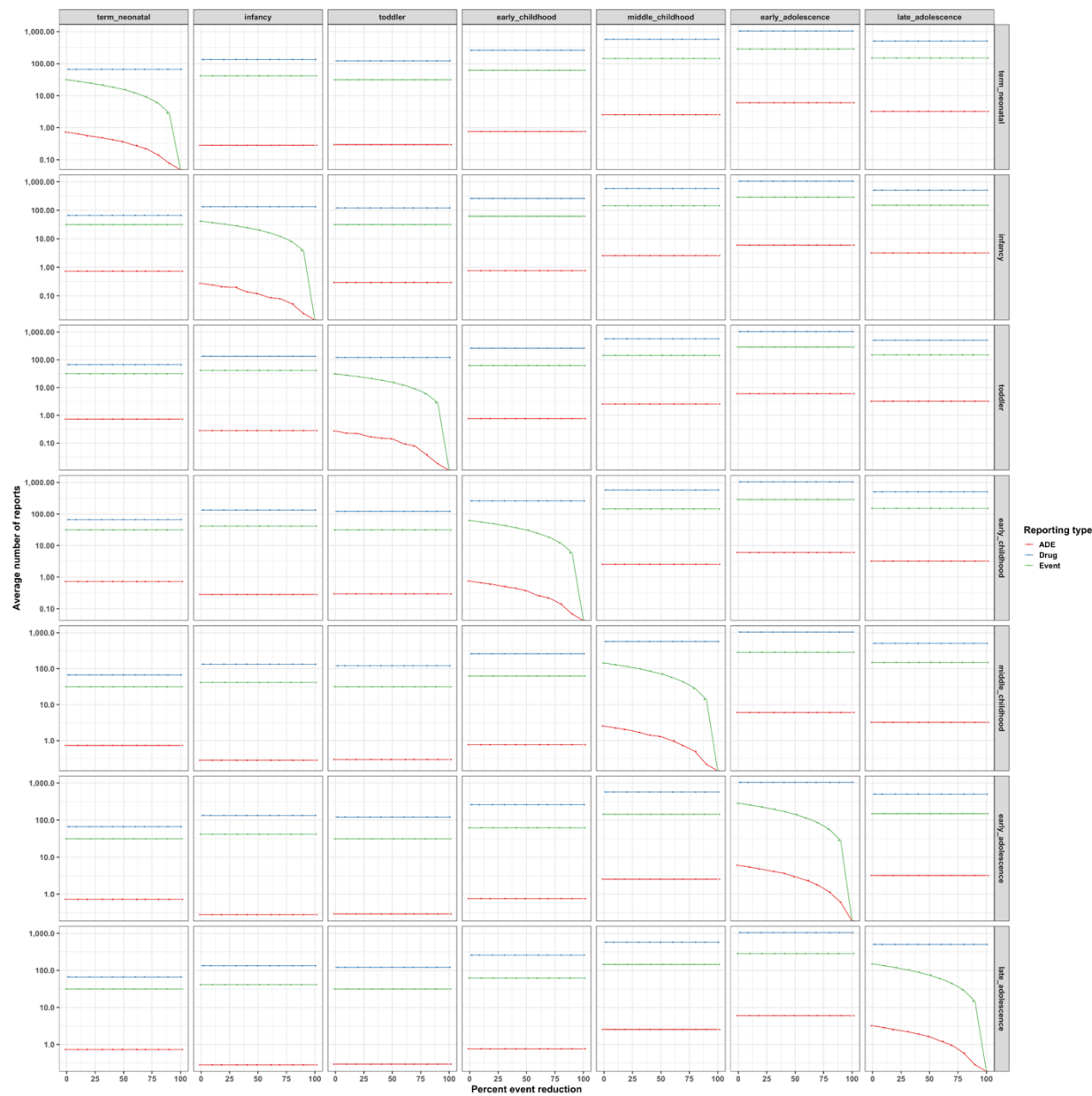


Fig. S4 Drug and event reporting as adverse events become rare at child development stages. The average number of drug, event, and drug event reports are shown at each child development stage as event reporting is reduced by 10% at each child development stage.

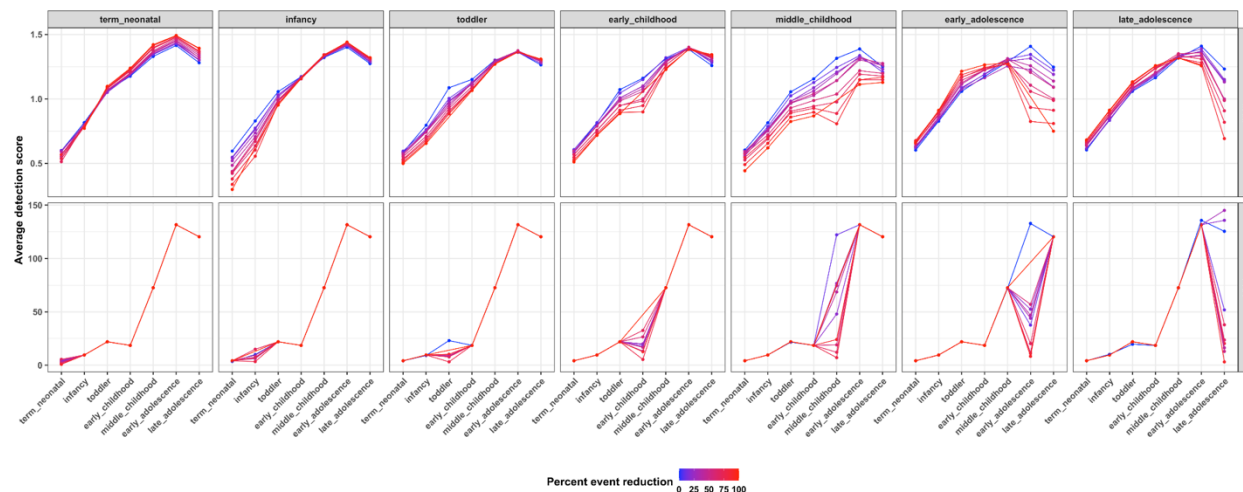


Fig. S5 GAM and PRR detection scores across childhood as adverse events become rare. The average ADE risk scores are shown at each child development stage as event reporting is reduced by 10% at each child development stage.

530

531

532

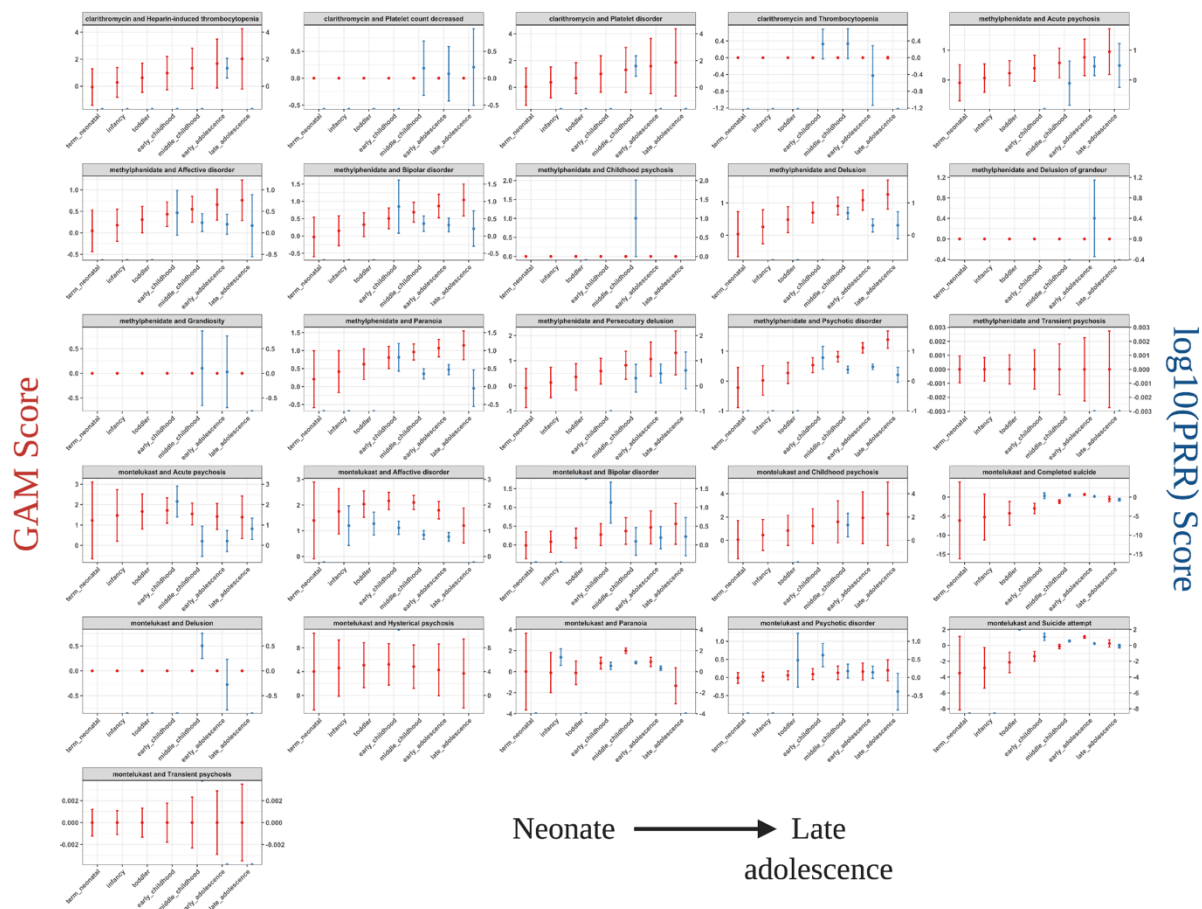


Fig. S6 GAM and PRR score comparison for real-world pediatric drug-events. Application of each ADE detection method on drug-event pairs from the clinically-validated GRiP pediatric reference set. The population score and 90% confidence interval are shown for each detection method. Only drug-event pairs with epidemiological or mechanistic evidence in children are shown.

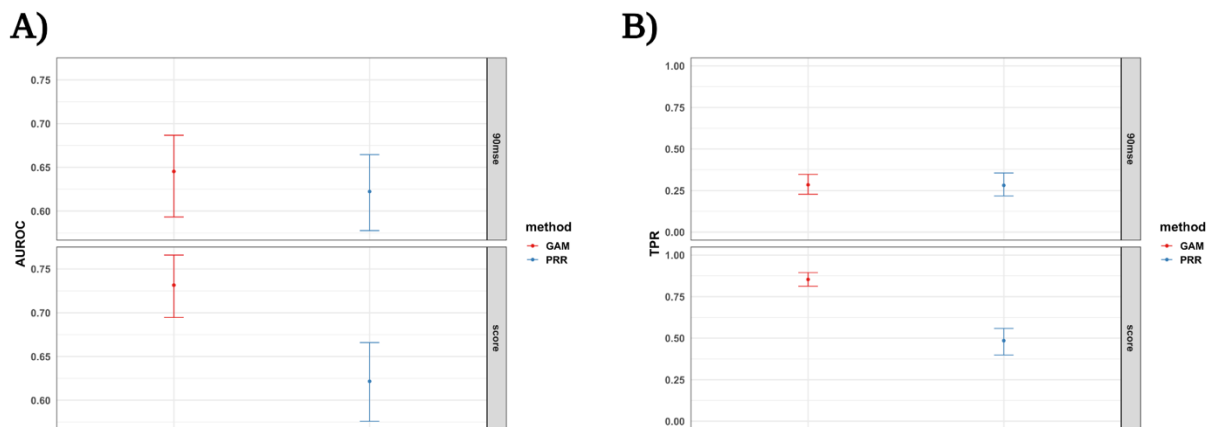


Fig. S7 GAM and PRR drug event real-world drug-event detection performance. A) The area under the receiver operating characteristic curve (AUROC) for detecting risk in real-world pediatric drug-event pairs. B) The true positive rate (TPR) for detecting risk in real-world pediatric drug-event pairs. Intervals represent the 95% confidence interval for the performance metric.

534

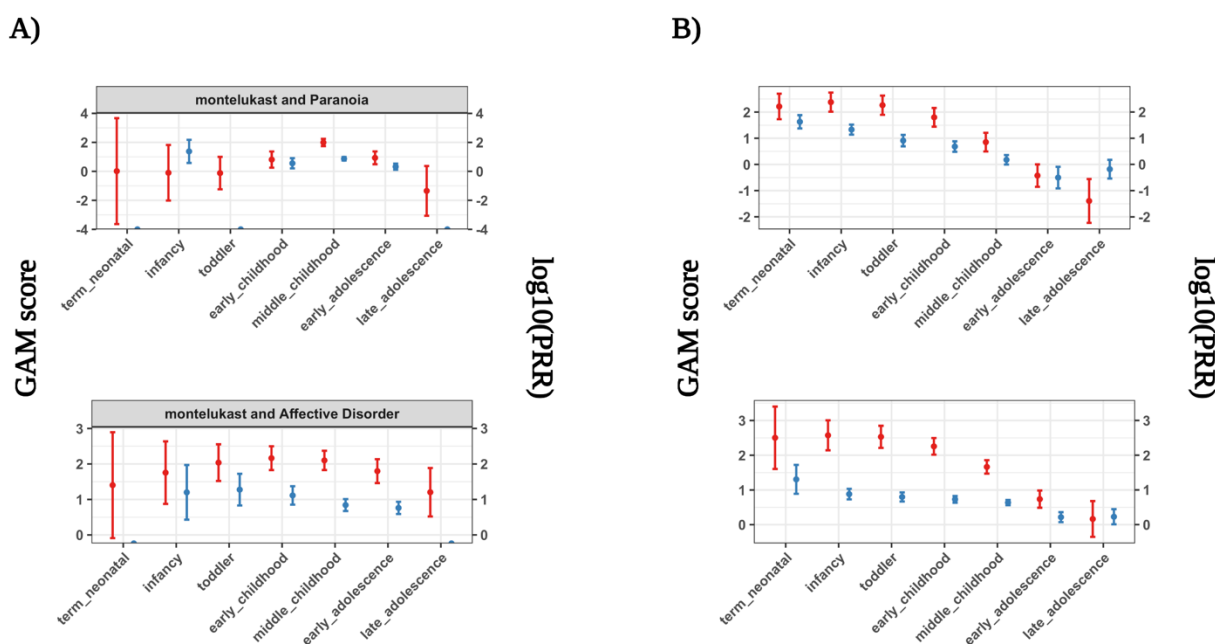


Fig. S8 GAM and PRR detection scores on sample real-world and simulated drug event data. We highlight two drug-event pairs from the A) real-world and B) simulated positive control set where scores across child development stages reflect dynamic ADE risks.

535

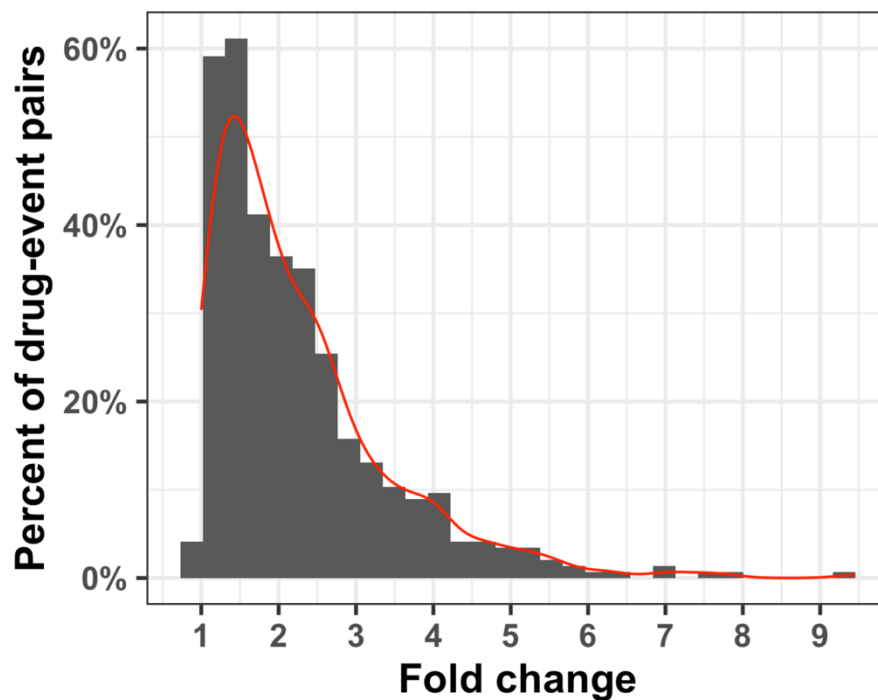


Fig. S9 Distribution of fold-changes for generating drug event dynamics of varying magnitudes. Distribution of fold-changes randomly assigned to drug-event pairs in the positive control set for each dynamics class.

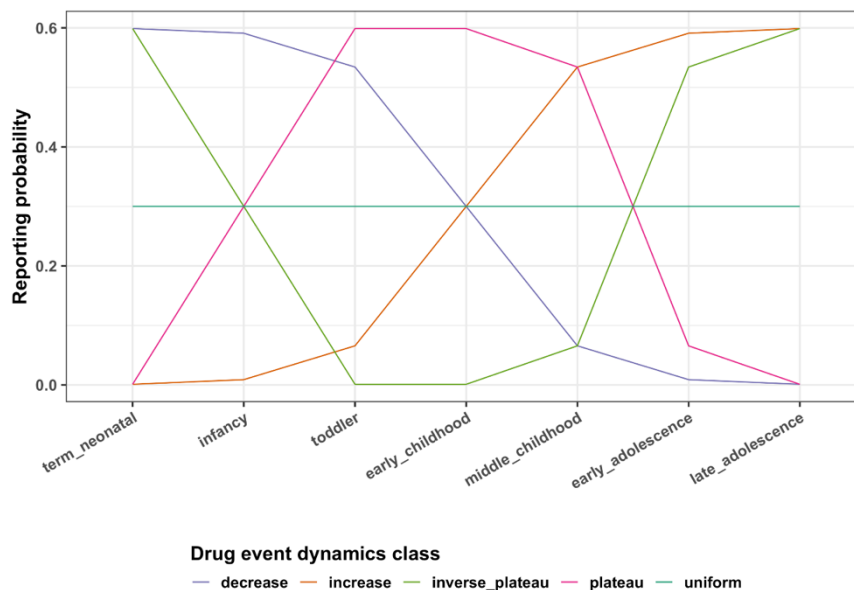


Fig. S10 Drug event reporting probability rates across child development stages. Each dynamics class represents a drug event reporting probability trend for drug-event pairs in the positive control set. An effect size, here 0.3, determined the magnitude of the drug event reporting dynamic. The average drug and event reporting across reports equaled the event reporting rate multiplied by a fold change factor resulting in the effect size of dynamic ADE reporting.

537
538
539
540
541
542
543
544
545
546
547
548
549

Table S1 High and low drug, event reporting at child development stages for across each dynamics class.

| Relative reporting rate within drug-event pairs at child development stages | | NICHD child development stages | | | | | | |
|---|-----------------|--------------------------------|---------|---------|-----------------|------------------|-------------------|------------------|
| | | Term neonatal | Infancy | Toddler | Early childhood | Middle childhood | Early adolescence | Late adolescence |
| Drug event dynamics classes | Decrease | High | High | NA | NA | NA | Low | Low |
| | Increase | Low | Low | NA | NA | NA | High | High |
| | Inverse Plateau | High | NA | Low | Low | Low | NA | High |
| | Plateau | Low | NA | High | High | High | NA | Low |
| | Uniform | NA | NA | NA | NA | NA | NA | NA |

550

551

Table S2 The number of drug-event pairs after the dynamics power analysis. Methods and scores had differences in drug reporting and effect size thresholds to identify drug, event pairs with atleast 80% power to differentiate scores between high and low reporting development stages.

| Number of drug-event pairs after the power analysis | | Drug event dynamics class | | | |
|---|-----------|---------------------------|-------------|-----------------|-------------|
| | | Decrease | Increase | Inverse Plateau | Plateau |
| Score | PRR | 282 (56.4%) | 283 (56.6%) | 282 (56.4%) | 282 (56.4%) |
| | PRR_90mse | 109 (21.8%) | 109 (21.8%) | 109 (21.8%) | 109 (21.8%) |
| | GAM | 109 (21.8%) | 109 (21.8%) | 109 (21.8%) | 109 (21.8%) |
| | GAM_90mse | 68 (13.6%) | 68 (13.6%) | 68 (13.6%) | 68 (13.6%) |

552

553

554